

Isospin of intermediate mass fragments produced in peripheral, midperipheral, and central collisions from the $^{58}\text{Ni}+^{12}\text{C}$, ^{24}Mg reactions at 34.5A MeV

Y. Larochelle,¹ L. Gingras,¹ G. C. Ball,^{2,*} L. Beaulieu,^{1,†} P. Gagné,^{1,‡} E. Hagberg,² Z. Y. He,¹ D. Horn,² R. Laforest,^{2,§} R. Roy,¹ and C. St-Pierre¹

¹Laboratoire de Physique Nucléaire, Département de Physique, Université Laval, Saint Foy, Québec, Canada G1K 7P4

²Chalk River Laboratories, Chalk River, Ontario, Canada K0J 1J0

(Received 12 June 2000; published 20 October 2000)

Isotopic yields of IMF's produced in the $^{58}\text{Ni}+^{12}\text{C}$, ^{24}Mg reactions at 34.5A MeV are investigated. Analysis of experimental data from the CRL-Laval 4π multidetector array focuses on events where at least 75% (60%) of the charge and momentum were detected for the $^{58}\text{Ni}+^{12}\text{C}$ ($^{58}\text{Ni}+^{24}\text{Mg}$) system. Averaged isospin ratios (N/Z) for IMF's with $Z=3$ and 4 are plotted as a function of emission angle and parallel velocity in the center-of-mass frame. Results from simulations with the statistical codes SMM and GEMINI, assuming an equilibrated source, are compared to the experimental ratios. The ratios seem to indicate the presence of a midrapidity necklike structure that would produce IMF's richer in neutrons than the two main emitters, even for very central collisions.

PACS number(s): 25.70.Lm, 25.70.Mn

The formation of a necklike structure between the two partners in a heavy ion collision at intermediate energies [1–6], even for light systems [7–11], is now a well established experimental phenomenon. However, many questions remain unanswered with respect to the dynamics involved in the formation of this necklike structure and its intrinsic characteristics, namely its density, isospin (in regards to the entrance channel), and size relative to the “spectator” nuclear matter remaining from quasiprojectile (QP) and quasitarget (QT). The mechanism leading to its breakup in light charged particles (LCP, $Z=1,2$) and intermediate mass fragments (IMF, $Z\geq 3$), and/or reabsorption by the collision partners, is also presently a hotly debated topic [12–15], especially with recent studies involving isospin measurement and its relation to (non)equilibrium phenomena [4,16,17]. Theoretical conjectures have suggested that because of neutron skin [18], clusterization of $N/Z=1$ clusters like deuterons and alphas [19] and the symmetry term effect on the nuclear potential [20], the isospin of the midrapidity region might be an important factor in the formation and breakup of a necklike structure.

On the other hand, several recent studies have shown that the hot nuclear system formed in the most central collisions between two heavy partners displays many characteristics of a thermalized and equilibrated source at high temperature [21,22], possibly undergoing a liquid-phase transition [23,24].

In this Rapid Communication, the similarities and differences, in regards to emission angle, particle velocity, and isospin ratio or “neutron-richness” (N/Z = neutron to proton ratio) between IMF's produced in peripheral, midperipheral, and central/fully-damped reactions are assessed. First, the experimental details, event selection, and analysis method are described. Then, using isotopic resolution for particles of charge $Z=3$ to 4, achieved with three Si-Si-CsI(Tl) telescopes in the CRL-Laval 4π multidetector array, the average IMF isospin ratios are plotted as a function of the angle of emission and the velocity in the center-of-mass frame (c.m.f.), along with results from filtered simulations assuming isospin equilibration. This is done for three different centrality cuts, based on the flow angle: peripheral, midperipheral (dissipative binary), and central (fully damped) collisions. Finally, the discussion and conclusions are presented with respect to the IMF production mechanisms that would induce the characteristics shown by the ratios extracted from the experimental results.

The experiments were performed at the Tandem Accelerator Superconducting Cyclotron (TASCC) facility of AECL at Chalk River. The CRL-Laval (Chalk River-Université Laval) 4π multidetector array [25–28] was used with a beam of ^{58}Ni at 34.5 MeV/nucleon impinging on ^{12}C (natural, 2.4 mg/cm²) and ^{24}Mg (enriched, 1.65 mg/cm²) targets. The CRL-Laval 4π array covers more than 80% of the solid angle around the target with ten rings of 12 to 16 modules, depending on the polar angle. The first four rings are made of plastic phoswiches with energy thresholds of 7.5 (27.5) MeV/nucleon for particles with charge $Z=1$ (28). The remaining six rings are made of CsI(Tl) crystal scintillators which achieve isotopic resolution for $Z=1,2$ and charge identification up to $Z=4$, with energy thresholds between 2 and 5 MeV/nucleon for $Z=1$ and 4, respectively. Finally three Si-Si-CsI(Tl) telescopes are inserted at angles of 15°, 20°, and 40° (rings 2, 3, and 5) in the setup. These telescopes achieved isotopic identification for up to $Z=4$ with thresholds from 2.0 to 3.1 MeV/nucleon. The electronic trigger during the experiment was a charged particle multiplicity of at least three particles.

*Present address: TRIUMF, 4004 Wesbrook Mall, Vancouver, British Columbia, Canada V6T 2A3.

†Present address: CHUQ, Hotel-Dieu de Québec, Service de Radio-oncologie et Centre de Recherche en Cancérologie de l'Université Laval, 11 Côte du Palais, Québec, Canada G1R 2J6.

‡Present address: Les Services Conseils Systématix, Inc., 830, Ernest-Gagnon, Edifice 4, Le Samuel-Holland, Bureau 201, Québec, Canada G1S 3R3.

§Present address: Mallinckrodt Institute of Radiology, 510 S. Kinghighway, St. Louis, MO 63110.

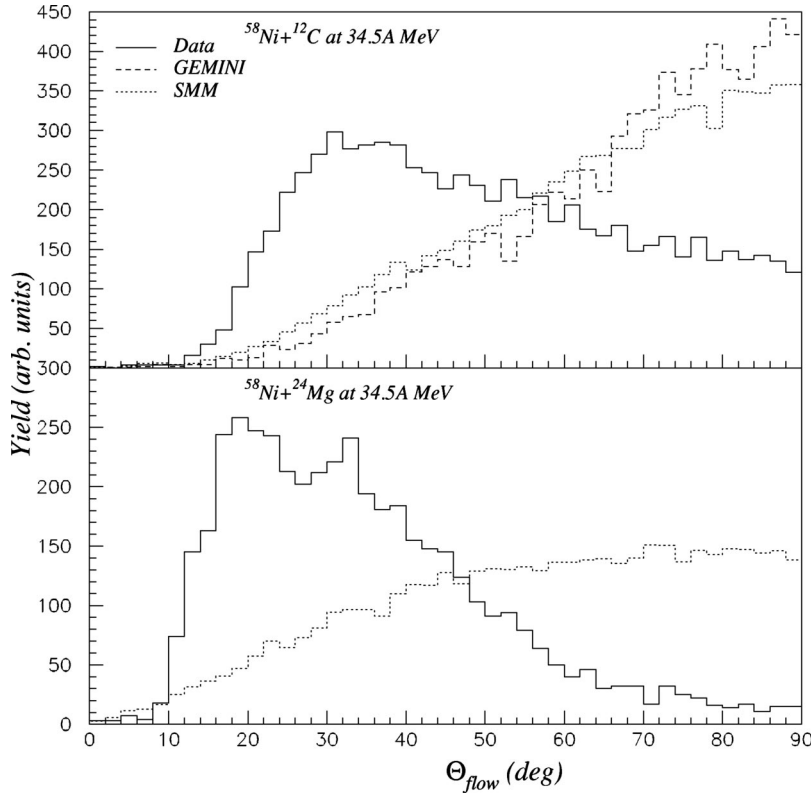


FIG. 1. Flow angle distributions for data (full line), filtered GEMINI simulations (dashed line), and SMM simulations (dotted line) for the reactions $^{58}\text{Ni}+^{12}\text{C}$ at 34.5A MeV (top) and $^{58}\text{Ni}+^{24}\text{Mg}$ at 34.5A MeV (bottom). Simulations are filtered with a software replica of the detector array and the counts are scaled to the data statistics.

In order to select different classes of events, in regards to their centrality (or binary) character, cuts on the flow angle (Θ_{flow}) were used for events where at least 75% (60%) of the charge and momentum of the whole system were detected for the $^{58}\text{Ni}+^{12}\text{C}$ ($^{58}\text{Ni}+^{24}\text{Mg}$) system. This last requirement suppresses mostly very peripheral events where deformation effects and nucleon exchange (isospin mixing) should be minimal. The flow angle method validity for event selection is well established from results published in previous papers [8,22,29,30], for which similar requirements on total charge have been applied.

The flow angle is defined from an event-shape tensor analysis in the calculated c.m.f., using the quadratic momentum tensor [31]:

$$P_{i,j}^2 = \sum_{n=1}^{N_{CP}} P_i^{(n)} P_j^{(n)}; \quad i,j=1,2,3, \quad (1)$$

where $P_i^{(n)}$, $P_j^{(n)}$ are the i th or j th Cartesian c.m.f. components of the particle momentum and N_{CP} is the total number of charged particles in the event. The three eigenvalues and eigenvectors calculated from this tensor define the shape of the event. The angle between the major axis of the event in momentum space (the eigenvector with the largest eigenvalue) and the beam axis is the flow angle.

A simulation with the code SMM [32,33] was performed to compare the experimental isospin ratios to an equilibrated, statistically decaying source. In SMM, all fragments are produced simultaneously and are driven apart by Coulomb repulsion, evocative of a prompt multifragmentation reaction mechanism. A complete fusion scenario was assumed, resulting in ^{70}Se ($^{58}\text{Ni}+^{12}\text{C}$) and ^{82}Zr ($^{58}\text{Ni}+^{24}\text{Mg}$) having an excitation energy equal to 343 MeV and 581 MeV, respec-

tively. The breakup volume ($V_{breakup} = 2.0 * V_0$) was chosen to give the best fit to the experimental charge distribution.

Simulations were also done with the statistical code GEMINI [34], which simulates sequential statistical emission with no Coulomb interaction between the fragments, with the same entrance channel as for SMM (excited ^{70}Se for the $^{58}\text{Ni}+^{12}\text{C}$ reaction) with a spin of $48\hbar$, the maximum spin this nucleus can sustain, following the prescription from Ref. [35].

The reaction products from the simulations were then filtered using a software replica of the geometry and energy thresholds of the CRL-Laval 4π multidetector. Double hits in a same module were rejected, and the same conditions as for the experimental data were used to select the events. Since both simulation codes assume a single fusion source, the two higher cuts of Θ_{flow} were favored. The effect of the experimental filter with this detector array is well understood from previous studies [8–10,27,28,36]: It essentially washes out very peripheral collisions, because the grazing angle of the reactions is smaller than the lower angle of the first ring of detectors. Simulations with GEMINI for the $^{58}\text{Ni}+^{24}\text{Mg}$ fusion channel (^{82}Zr) produce insufficient filtered statistics, when requiring detection of an IMF in a Si-Si-CsI(Tl) telescope, and were excluded from the analysis. This was mainly due to the higher excitation energy and lower c.m.f. velocity for that system (in regards to the detection energy thresholds), and the lower IMF production rate in GEMINI, when compared to either the data or to SMM.

Figure 1 shows flow angle distributions for experimental data and filtered simulations. As previously observed for isotropic emission, both single-source simulations are very similar to each other and show a sinelike distribution, peak-

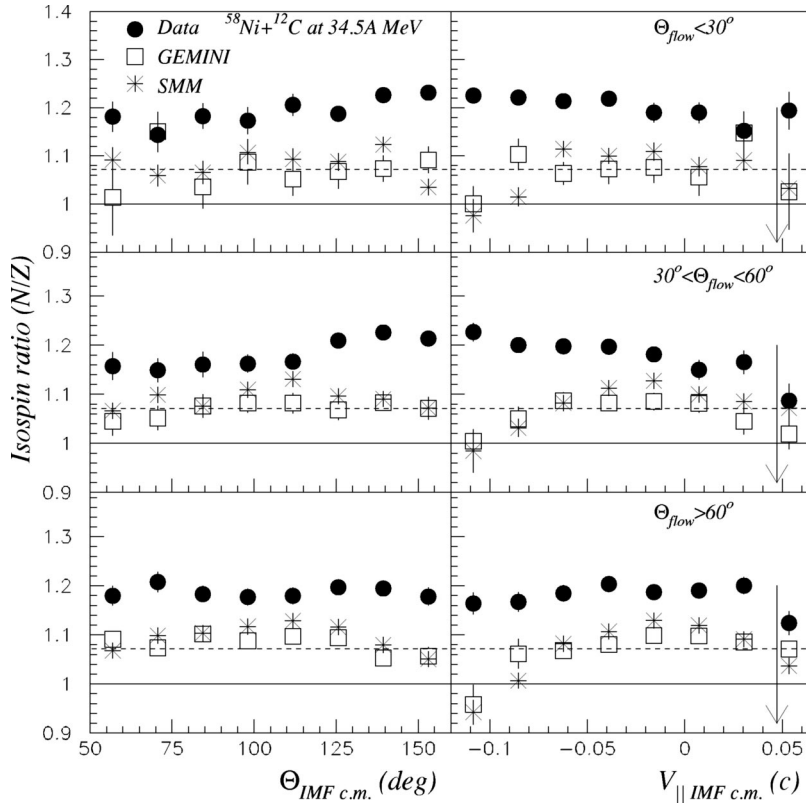


FIG. 2. Average isospin ratios (N/Z) for well identified IMF's with $Z=3$ or 4 as a function of the emission angle in the center-of-mass reference frame (left) and the center-of-mass particle velocity parallel to the beam axis (right) for the reaction $^{58}\text{Ni}+^{12}\text{C}$ at $34.5A$ MeV (full dots). Cuts are made on $\Theta_{flow} < 30^\circ$ (top), $30^\circ < \Theta_{flow} < 60^\circ$ (middle), and $\Theta_{flow} > 60^\circ$ (bottom). Open boxes represent filtered GEMINI simulations and stars are results from filtered SMM simulations (see text). Error bars are the statistical errors for a given angle or velocity bin. When no error bar is present, the error is smaller than the size of the symbol. The dotted lines show the isospin ratio for ^{58}Ni (1.07) and the full line for ^{12}C (1.00). The arrow shows the velocity of the ^{58}Ni projectile in the center-of-mass frame for the $^{58}\text{Ni}+^{12}\text{C}$ reaction.

ing at $\Theta_{flow} = 90^\circ$ [8,29]. The experimental distribution, however, peaks at around 30° and only very few events have a $\Theta_{flow} > 60^\circ$, indicating that most of the cross section is made of dissipative binary events and necklike structure formation, as established previously [8–11,27,28]. Because the total mass and momentum requirements for the two systems are different, the $^{58}\text{Ni}+^{12}\text{C}$ distribution shows more counts for a higher value of Θ_{flow} than the $^{58}\text{Ni}+^{24}\text{Mg}$ distribution. Since the purpose of the simulations was to obtain the isotopic distributions of equilibrated sources, the simulations were done for single-source events and hence do not reproduce the contribution to the flow-angle distributions at small angles expected from a binarylike reaction.

To assess the neutron richness of the reaction products from different dynamical or statistical “source(s),” isospin ratios are analyzed as a function of the emission angle, relative to the beam axis, and the isotope velocity in the c.m.f. Because IMF isotopic resolution is only achieved in the three Si-Si-CsI(Tl) telescopes, situated at high angle in the c.m.f., the distributions are limited to particles emitted from 50° to 160° and to velocity from $\approx -0.1c$ to $0.1c$ in the c.m.f., hence including midrapidity emission for the asymmetric $^{58}\text{Ni}+^{12}\text{C}(^{24}\text{Mg})$ systems.

Emission from an isotopically equilibrated source, either spherical or deformed, or from a purely binary dissipative collision should produce a flat distribution of isospin ratios for both the angular and velocity distributions. Unfiltered results from both simulations confirm that prediction. Unfiltered SMM simulations are showing a small average isospin ratio drop at higher parallel velocity, possibly because of the bigger Coulomb push for lighter isotopes (lower N/Z). Besides, identification thresholds for the different charges and

isotopes are different in the telescopes, namely the lighter isotopes are identified at lower energies than the heavier ones. Hence differences arise in the average isospin ratio distributions for the lower velocities along the parallel velocity axis for the filtered simulations, as shown hereafter.

On the other hand, it has been shown that semiperipheral collisions can often lead to the formation of a necklike structure between the two main emitters [1–5,8]. In those dynamically driven events, isospin equilibrium is not necessarily achieved. It has been hinted that because of rapid clusterization of light $N/Z=1$ particles [19] and/or driving force caused by the nuclear potential symmetry term [20], neutron enrichment occurs for particles emitted in the midrapidity region. Enhancement of neutron-rich isotopes has been observed experimentally at midrapidity [4,16].

In the present data set, such effects should produce a higher N/Z ratio value in the midrapidity region (around $0.0c$ in the c.m.f. and also regions in velocity space at higher c.m.f. angles, because of the Coulomb push of the ^{58}Ni -derived QP on the neck) than in the equilibrated simulations.

In the next two figures, the average isospin ratios of IMF's with $Z=3$ or 4 are shown for the $^{58}\text{Ni}+^{12}\text{C}$ (Fig. 2) and $^{58}\text{Ni}+^{28}\text{Mg}$ at $34.5A$ MeV (Fig. 3) reactions, along with the results from the SMM and GEMINI simulations for both systems for three cuts on Θ_{flow} . The cuts define peripheral ($\Theta_{flow} < 30^\circ$), dissipative binary ($30^\circ < \Theta_{flow} < 60^\circ$) and central/fully-damped events ($\Theta_{flow} > 60^\circ$). As shown previously [8,22,29,30], the cut on high values of Θ_{flow} seems to isolate seemingly single-source events from the clearly binary/peripheral events ($\Theta_{flow} < 30^\circ$) and the dissipative bi-

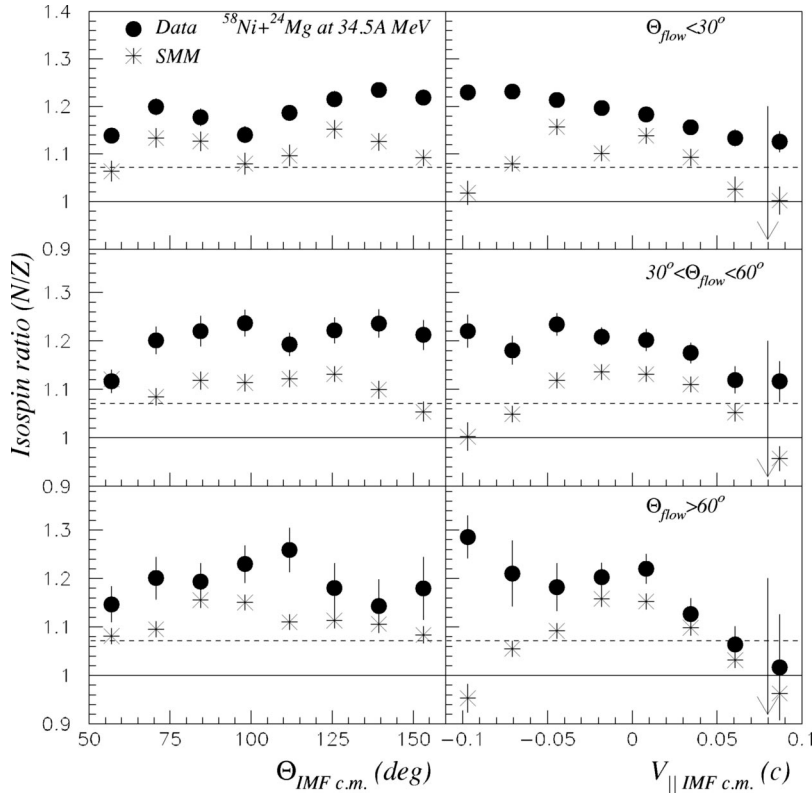


FIG. 3. Same as Fig. 2, but for the reaction $^{58}\text{Ni}+^{24}\text{Mg}$ at 34.5A MeV, and without the GEMINI simulations (see text). The dotted lines show the isospin ratio for ^{58}Ni (1.07) and the full line for ^{24}Mg (1.00). The arrow shows the velocity of the ^{58}Ni projectile in the center-of-mass frame for the $^{58}\text{Ni}+^{24}\text{Mg}$ reaction.

nary events ($30^\circ < \Theta_{flow} < 60^\circ$), where midrapidity emission seems to be the most important [2,4,5,8]. The ratios are plotted against the emission angle and the parallel velocity in the c.m.f.

For both systems, the average isospin ratio for the experimental data shows the same trend for all cuts on Θ_{flow} : An IMF isospin ratio value close to that of ^{58}Ni (1.07) near the beam velocity and a clearly higher average IMF isospin ratio value than both simulations at low parallel velocity and at large angle in the c.m.f. These are the characteristics for the emission of IMF's richer in neutrons in the midrapidity zone, possibly originating from a necklike structure breakup, followed by the Coulomb push of the QP. There is a small deviation for the $^{58}\text{Ni}+^{12}\text{C}$ case at $\Theta_{flow} < 30^\circ$, where the N/Z averaged ratio in the last data bin at high parallel velocity tends to go up. Since the most peripheral collisions are suppressed by the experimental setup, this might result from lower statistics for that channel.

The filtered SMM and GEMINI simulations, in contrast, show an almost flat distribution for the full range of emission angles. This is expected for isotropic emission from an equilibrated source. The lower ratio value at smaller velocities for distribution of average isospin ratios versus IMF parallel velocity, seen in both simulations, is a result of the identification threshold differences in the telescopes for $Z = 3,4$ isotopes for the lower velocity, as discussed above. Both simulations give very similar distributions, not reproduced by the experimental data, which show more isospin enhancement at low velocity and large angle.

The surprising result for events with $\Theta_{flow} > 60^\circ$ is that even if the emission pattern for experimental data from those events closely resembles that of a single-source, as shown in

Refs. [8,22,29,30], the isospin ratios are clearly different from the single-source simulations. This could mean that even though there is almost complete damping of the two reaction partners, complete fusion is not achieved, as observed recently for a heavier system [15], and a participant zone or necklike structure is still present in the midrapidity region, that zone producing IMF's richer in neutrons. Similar observations of nonequilibrium (in regards to isospin) in central heavy-ion collisions were reported recently for a symmetric total system of ≈ 200 nucleons at a beam energy of 400 MeV/nucleon [17]. It should also be noted that the experimental average isospin ratio value is systematically higher than that of the simulations, which is always very close to that of ^{58}Ni (1.07), for the whole angular and velocity range analyzed here. This could mean that dynamical IMF emission differs (at least in its isospin) from theoretical assumption of single-source equilibrated nuclear matter.

In conclusion, experimental events from the $^{58}\text{Ni}+^{12}\text{C}$, ^{24}Mg reactions at 34.5A MeV detected with the CRL-Laval 4π multidetector array were selected where at least 75% and 60% of the charge and momentum were recovered for both systems, respectively. Cuts on the flow angle were used to differentiate between peripheral, dissipative binary, and central/fully damped reactions. Isospin ratios (N/Z) were plotted as a function of emission angle and parallel velocity in the c.m.f. Products from filtered SMM and GEMINI simulations of a completely equilibrated fusion scenario were analyzed in the same way. The ratios seem to exhibit characteristics compatible with the formation (and breakup) of a neutron-rich necklike structure between the two main emitters, even for collisions previously deemed as "single-source" ($\Theta_{flow} > 60^\circ$). It is also important to note that

neutron-skin effects [18,20] should be almost nonexistent for small isospin-symmetric nuclei like ^{58}Ni and especially ^{12}C and ^{24}Mg .

Besides, recent results with a heavier system ($^{129}\text{Xe} + ^{120}\text{Sn}$) [37] have shown that the N/Z ratio of the midrapidity material is indistinguishable from that of the entire system. For the present analysis, however, the high N/Z ratio of the IMF's at midrapidity and the small size of the system seem to indicate a higher N/Z ratio for the midrapidity zone than for the total system. Differences in mass or mass asymmetry of the systems, could explain the apparent disparity in the measurements.

The present results would be consistent with a hypothesis previously reported [9,10,27,28] where the two reaction partners colliding at a beam energy between ≈ 20 and 50 MeV/nucleon first undergo an important deformation, leading to the formation of a necklike structure between them. This neck would favor the transfer of nucleons from the heavier

partner to the lighter one in a mass-asymmetric reaction (symmetrization [9,38]). In such a case, neutron enrichment in the midrapidity zone would occur before a fast neck rupture, possibly because of the longer timescale involved in overcoming the Coulomb barrier for protons. Isospin-asymmetry term in the nuclear potential would also favor the neutron enrichment of a low density region (neck) [20,39]. Then, after the neck breakup and/or its reabsorption by one or both emitters, the remaining excited system(s) would decay following a thermodynamical (statistical) pattern. It would be interesting to compare recent experimental results to simulations assuming such a reaction mechanism.

We would like to thank R.J. Charity and A.S. Botvina for the use of their statistical codes. This work was supported in part by the Natural Sciences and Engineering Research Council of Canada and the Fonds pour la Formation de Chercheurs et l'Aide à la Recherche du Québec.

-
- [1] C.P. Montoya *et al.*, Phys. Rev. Lett. **73**, 3070 (1994).
 [2] J. Tóke *et al.*, Phys. Rev. Lett. **75**, 2920 (1995).
 [3] J.F. Lecomte *et al.*, Phys. Lett. B **354**, 202 (1995).
 [4] J.F. Dempsey *et al.*, Phys. Rev. C **54**, 1710 (1996).
 [5] J. Lukasik *et al.*, Phys. Rev. C **55**, 1906 (1997).
 [6] Ph. Eudes *et al.*, Phys. Rev. C **56**, 2003 (1997).
 [7] J. Peter *et al.*, Nucl. Phys. **A593**, 95 (1995).
 [8] Y. Larochelle *et al.*, Phys. Rev. C **55**, 1869 (1997).
 [9] Y. Larochelle *et al.*, Phys. Rev. C **57**, R1027 (1998).
 [10] Y. Larochelle *et al.*, Phys. Rev. C **59**, R565 (1999).
 [11] T. Lefort *et al.*, Nucl. Phys. **A662**, 397 (2000).
 [12] D. Durand, Nucl. Phys. **A630**, 52c (1998), and references therein.
 [13] B. Tamain *et al.*, Multifragmentation: Proceedings of the International Workshop XXVII on Gross Properties of Nuclei and Nuclear Excitations, Hirschegg, Austria, 1999, p. 12.
 [14] L.G. Sobotka, Multifragmentation: Proceedings of the International Workshop of Gross Properties of Nuclei and Nuclear Excitations [13], p. 72.
 [15] R. Nebauer *et al.*, Nucl. Phys. **A658**, 67 (1999).
 [16] R. Laforest *et al.*, Phys. Rev. C **59**, 2567 (1999).
 [17] F. Rami *et al.*, Phys. Rev. Lett. **84**, 1120 (2000).
 [18] L. G. Sobotka, Phys. Rev. C **50**, R1272 (1994).
 [19] L.G. Sobotka *et al.*, Phys. Rev. C **55**, 2109 (1997).
 [20] M. Colonna *et al.*, Phys. Rev. C **57**, 1410 (1998).
 [21] M. D'Agostino *et al.*, Phys. Lett. B **371**, 175 (1996).
 [22] N. Marie *et al.*, Phys. Lett. B **391**, 15 (1997).
 [23] M.L. Gilkes *et al.*, Phys. Rev. Lett. **73**, 1590 (1994).
 [24] J. Pochodzalla *et al.*, Phys. Rev. Lett. **75**, 1040 (1995).
 [25] C. Pruneau *et al.*, Nucl. Instrum. Methods Phys. Res. A **297**, 404 (1990).
 [26] Y. Larochelle *et al.*, Nucl. Instrum. Methods Phys. Res. A **348**, 167 (1994).
 [27] L. Gingras *et al.*, "Quasi-projectile formation and decay comparisons between $^{58}\text{Ni}+\text{C}$ and $^{58}\text{Ni}+\text{Au}$ reactions at 34.5A MeV," in *Advance in Nuclear Dynamics 3: Proceedings of the 13th Winter Workshop on Dynamics, Marathon, Florida Keys, 1997*, edited by W. Bauer (Plenum, New York, 1997).
 [28] L. Gingras *et al.*, in *Proceedings of the XXXVIth Winter Meeting on Nuclear Physics, Bormio, Italy, 1998*, edited by I. Iori, p. 361.
 [29] L. Beaulieu *et al.*, Phys. Rev. Lett. **77**, 462 (1996).
 [30] N. Marie *et al.*, Phys. Rev. C **58**, 256 (1998).
 [31] J. Cugnon and D. L'Hôte, Nucl. Phys. **A397**, 519 (1983).
 [32] A.S. Botvina *et al.*, Nucl. Phys. **A475**, 663 (1987).
 [33] A.S. Botvina *et al.*, Nucl. Phys. **A507**, 649 (1990).
 [34] R.J. Charity *et al.*, Nucl. Phys. **A483**, 371 (1988); computer code GEMINI obtained from Wunmr.wustl.edu via anonymous FTP.
 [35] R. Schmidt and H.O. Lutz, Phys. Rev. A **45**, 7981 (1992).
 [36] Y. Larochelle *et al.*, Phys. Rev. C **53**, 823 (1996).
 [37] L.G. Sobotka *et al.*, Phys. Rev. C **62**, 031 603 (2000).
 [38] G. Casini *et al.*, Phys. Rev. Lett. **83**, 2537 (1999).
 [39] H. Müller and B.D. Serot, Phys. Rev. C **52**, 2072 (1995).